

# Ising Models of Cooperativity in Muscle Contraction

Elaheh Saadat,<sup>1</sup> Matthieu Caruel,<sup>2</sup> Stefano Gherardini,<sup>3</sup> Ilaria Morotti,<sup>4,5</sup> Matteo Marcello,<sup>4,5</sup> Marco Caremani,<sup>4,5</sup> Marco Linari,<sup>4,5</sup> Ivan Latella,<sup>6,7</sup> and Stefano Ruffo<sup>1,8</sup>

<sup>1</sup>SISSA, via Bonomea 265 and INFN, Sezione di Trieste, 34136 Trieste, Italy

<sup>2</sup>Univ Paris Est Creteil, Univ Gustave Eiffel, CNRS, UMR 8208, MSME, F-94010 Créteil, France\*

<sup>3</sup>Istituto Nazionale di Ottica del Consiglio Nazionale delle Ricerche (CNR-INO), Largo Enrico Fermi 6, I-50125 Firenze, Italy<sup>†</sup>

<sup>4</sup>Department of Biology, University of Florence, I-50019 Sesto Fiorentino, Italy

<sup>5</sup>PhysioLab, University of Florence, I-50019 Sesto Fiorentino, Italy

<sup>6</sup>Departament de Física de la Matèria Condensada,

Universitat de Barcelona, Martí i Franquès 1, 08028 Barcelona, Spain

<sup>7</sup>Institut de Nanociència i Nanotecnologia de la Universitat de Barcelona (IN2UB), Diagonal 645, 08028 Barcelona, Spain<sup>‡</sup>

<sup>8</sup>Istituto dei Sistemi Complessi, Consiglio Nazionale delle Ricerche,  
Via Madonna del Piano 10, 50019 Sesto Fiorentino, Italy<sup>§</sup>

Regulation of contraction in striated muscle is controlled by a dual mechanism involving both thin filaments containing actin and thick filaments containing myosin. The thin filament is activated by calcium ions binding to troponin, leading to tropomyosin azimuthal displacement which allows the activation of a regulatory unit (composed of one troponin, one tropomyosin and seven actin monomers) that exposes the actin sites for interaction with the myosin motors. Motor attachment to actin contributes to spreading activation within and beyond a regulatory unit along the thin filament through a cooperative mechanism. We introduce a one-dimensional Ising model to elucidate the mechanism of cooperativity in thin filament activation in relation to the force generated by the attached myosin motor. The model characterizes thin filament activation and cooperativity using only two parameters: one related to calcium concentration and the other to the force exerted by the attached myosin motor, which is modulated by temperature. At any force, the model is able to determine the extent of actin-myosin interactions on a correlation length ranging from two to seven actin monomers in addition to the seven actin monomers of the regulatory unit. Our theoretical predictions are successfully tested on experimental data, and our tests also include the condition of hindered filament activation by the use of the specific drug Omecamtiv Mecarbil (OM). According to our model, the effect of OM results in an anti-cooperativity mechanism accounting for the experimental data.

## I. INTRODUCTION

In the striated muscle cell, steady force and shortening is due to two bipolar arrays of the motor protein myosin II emerging from the backbone of the thick filament. The arrays of myosin motors pull the thin actin-containing filaments towards the center of the sarcomere, the  $\sim 2\ \mu\text{m}$ -long structural unit of striated muscle, during cyclical ATP-driven interactions [1], as shown in Fig. 1[(a)-(b)]. In the resting muscle, contraction is prevented by the regulatory protein tropomyosin (Tm) in the thin filament that masks the actin sites for myosin binding [2]. Contraction is also prevented by the autoinhibition that operates in the myosin motors in the OFF state, in which the motors lie on the surface of the thick filament folded on their tail toward the center of the sarcomere unable to bind actin and hydrolyze ATP [3, 4]. Upon stimulation,  $\text{Ca}^{2+}$  is released from the sarcoplasmic reticulum and binds to the regulatory protein troponin C (TnC) of the troponin complex (Tn) on the thin filament.

This allows for an azimuthal displacement of Tm that exposes the actin sites for the interactions with the myosin motors [5]. During loaded contractions, the stress generated by few constitutively ON motors in the thick filament would allow the OFF motors to be switched ON [6–9]. Thick filament mechanosensing is likely mediated by titin that, upon stimulation, has recently been shown to become an efficient mechanical coupler at physiological sarcomere length [10, 11].

Along the thin filament,  $\text{Ca}^{2+}$  binding to TnC allows the activation of regulatory units (RUs). For each strand of the double-stranded helix, a RU is composed of seven actin monomers, one Tn complex and one Tm. Activation can spread beyond a RU for the head-tail interactions between consecutive Tm's, suggesting a cooperative mechanism of thin filament activation. Experimental evidence shows that strong attachment of the myosin motor to actin is responsible for full actin sites availability [12–15]. This supports a two-step steric-blocking model of thin filament activation [16]. During the first step,  $\text{Ca}^{2+}$  binding to TnC is responsible for partial displacement of Tm (blocked-to-closed transition) that, within one RU, allows myosin to establish weak interactions with the actin. The second step is triggered by the weak-to strong transition of myosin-actin interaction that further promotes Tm displacement (closed-to-open transition), which may provide the cooperative mecha-

\* matthieu.caruel@u-pec.fr

† stefano.gherardini@ino.cnr.it

‡ ilatella@ub.edu

§ ruffo@sissa.it

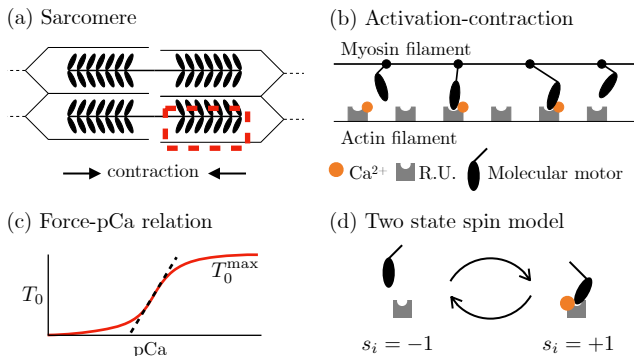


Figure 1. (a) Schematic of a muscle sarcomere. The red rectangle surrounds interacting myosin and actin filaments. (b) Activation-contraction mechanism:  $\text{Ca}^{2+}$  ions bind to regulatory units (RUs) to allow molecular motor attachment and force generation; we stress that the RUs are only pictorially represented. (c) Typical force-pCa relation (red continuous line). The maximum slope of the relation (black dashed line), associated to the Hill coefficient  $n_H$ , quantifies the degree of cooperativity. (d) Two-state Ising model used in this paper.

nism for spreading thin filament activation beyond the RU [17–19].

The modulation of the muscle contraction by calcium can be characterized by the relation between the  $\text{Ca}^{2+}$  concentration ( $[\text{Ca}^{2+}]$ ) and the steady force  $T_0$  generated in isometric conditions by demembrated muscle fibers at a given sarcomere length [20]. This dependence of the force on the  $[\text{Ca}^{2+}]$  is represented by the so-called *force-pCa relation* where  $\text{pCa} = -\log_{10}([\text{Ca}^{2+}])$ , see Fig. 1(c).

As in various biological regulatory processes, the relation between the activation input (pCa) and its output ( $T_0$ ) is highly non-linear showing a sharp sigmoidal transition between all or none states. Denoting  $T_0^{\max}$  the isometric force measured at saturating  $[\text{Ca}^{2+}]$ , the normalized force  $f = T_0/T_0^{\max}$  is often conventionally associated with the Hill function [21], i.e.,

$$f = \frac{1}{1 + c^{-n_H}}, \quad (1)$$

where  $c = [\text{Ca}^{2+}]/[\text{Ca}^{2+}]_{50}$ , such that  $T_0 = T_0^{\max}/2$  when  $c = 1$ . The exponent  $n_H$ , called the Hill coefficient, represents the cooperativity degree of the activation process, which can be associated with the slope of the force-pCa relation around  $[\text{Ca}^{2+}] = [\text{Ca}^{2+}]_{50}$ , as shown in Fig. 1(c). A high cooperativity translates into a sharp increase of the tension upon a small change in the calcium concentration.

Recently, Caremani et al. [19] reported that  $n_H$  increases proportionally with the force  $F_0$  exerted by a myosin motor attached to actin; such a force is modulated by temperature. This observation suggests that the force produced by the attached motors may enhance the activation of neighboring regulatory units without the help of extra calcium binding. This mechanistic explanation

of the observed increase in cooperativity with  $F_0$  is supported by measurement of the force-pCa relation in the presence of the positive inotrope Omecamtiv Mecarbil (OM) [22, 23]. OM is a small molecule that suppresses the myosin working stroke and prolongs the lifetime of the myosin-actin attachment at physiological ATP concentrations and at therapeutic OM concentrations [23–25]. In the presence of OM,  $n_H$  shows a shallower slope of the force-pCa relation, which may be attributed to OM-bound motors failing to generate force [24, 25].

The objective of this paper is to provide a physical model that is able to validate this interpretation of the experimental results, by providing also quantitative predictions that may stimulate further experiments. For this purpose, we use a statistical mechanical approach based on the classical one-dimensional Ising model. The aim of our approach is to evaluate the effect of temperature and of the presence of OM on the parameters used in the one-dimensional Ising model to quantify cooperativity in isometric steady state conditions. Because of its simplicity, this model is insufficient to describe experimental data underpinning the current understanding of the molecular processes behind muscle contraction. More comprehensive models can be found in Refs. [26–36]. In the current literature, an Ising-like model of thin filament activation was formulated by Rice et al. [37], who considered a model of spins structured in two layers, where each unit of the model represents a RU. The first layer of spins identifies the presence of absence of  $\text{Ca}^{2+}$  on the RU, while the second layer describes whether the RU is occupied by a force generating myosin motor.

In the present work, we show that the force-pCa relations measured experimentally by Caremani et al. [19] can be well-reproduced already with a single-layer Ising spin model, see Fig. 1(d). We relate the change in the degree of cooperativity, observed at different temperatures and in the presence/absence of OM, to the change in the spread of thin filament activation between neighboring RUs. In particular, a large cooperativity suggests a molecular process by which the number of RU activated by a  $\text{Ca}^{2+}$  ion can be larger than one through head-tail interactions between neighboring Tn-Tm complexes, as previously suggested by Regnier et al. [38].

Moreover, we establish a bijective relationship between the Hill coefficient and the coupling constant of the single-spin Ising model, which can be interpreted as an effective measure of cooperativity at the molecular scale. We show that a modulation of this coupling constant accounts for the dependence of the Hill coefficient on the motor force  $F_0$  observed experimentally in [19]. Furthermore, the computation of the correlation length of the Ising model indicates that the range of these interactions increases with  $F_0$  and is of the order of one to two regulatory units, which supports the mechanistic model proposed in [19]. We also obtain that larger temperatures correlate with stronger nearest-neighbor interactions of the model.

Finally, we quantitatively compare our results with the

former work by Rice et al. [37]. While their model was expected to take into account more faithfully the physiological activation mechanism, we show that it is over-determined, at least in the context set by the available data on force-pCa relations obtained on skeletal muscle. Moreover, we demonstrate that the Rice et al. model cannot be calibrated to reproduce simultaneously, with the same non-degenerate set of parameters, the behaviors of the force-pCa relations observed at high and low calcium concentrations.

## II. TWO-STATE ISING MODEL

We consider a one-dimensional chain of  $N$  force generating units with nearest-neighbor interactions. Each unit represents an actin-myosin complex that can be in two states: *non-force generating* in which no  $\text{Ca}^{2+}$  is bound and the motor is detached, or *force generating* in which  $\text{Ca}^{2+}$  is bound and a myosin motor is attached and produces force. The state of unit  $i \in \{1, \dots, N\}$  is characterized by a discrete variable (spin)  $s_i \in \{-1, +1\}$ , where  $s_i = +1$  (respectively  $-1$ ) corresponds to the force generating (respectively non-force generating) state, see Fig. 1[(b) and (d)].

In the following, we consider that the parameters entering our model are dimensionless, with all energy quantities being rescaled by the thermal energy  $k_B T$ . As suggested by the experimental study conducted in [19], we introduce a dimensionless coupling constant  $J$  characterizing the strength of nearest-neighbor interactions. We denote by  $h$  the dimensionless external field, accounting for the concentration of  $\text{Ca}^{2+}$ , and write the Hamiltonian of the system as

$$H_1 = - \sum_{i=1}^N (J s_i s_{i+1} + h s_i), \quad (2)$$

with periodic boundary conditions. Following the approach used by [39] and [40], the spin model can be associated with a two-state Markov process with transition rates  $k_{\pm}^i$ . This mapping reads as

$$s_i = -1 \xrightleftharpoons[k_-^i]{k_+^i} s_i = +1, \quad \forall i \in \{1, \dots, N\},$$

where the transition rates  $k_{\pm}^i$  linked to the  $i$ th unit verify the detailed balance condition

$$\begin{aligned} \frac{k_+^i}{k_-^i} &= \exp \left\{ - [H_1(s_i = +1) - H_1(s_i = -1)] \right\} = \\ &= \exp \left\{ 2 [J (s_{i+1} + s_{i-1}) + h] \right\}. \end{aligned} \quad (3)$$

To compare our model predictions with the experimental results, we associate (i) the external field  $h$  to the normalized intracellular calcium concentration  $c$  and (ii) the coupling  $J$  to the Hill coefficient  $n_H$  using the identities

$$h = \frac{1}{2} \log(c), \quad J = \frac{1}{2} \log(n_H). \quad (4)$$

With these notations, the detailed balance condition (3) becomes

$$\frac{k_+^i}{k_-^i} = c n_H^{(s_{i+1} + s_{i-1})}. \quad (5)$$

### A. Force-pCa relation

Quantities of interest in the one-dimensional Ising model can be obtained using the standard transfer matrix method.[41] For instance, the magnetization per spin is given by

$$\langle s \rangle = \frac{\sinh(h)}{[\sinh^2(h) + e^{-4J}]^{1/2}}, \quad (6)$$

which ranges in the interval  $[-1, 1]$ . Considering that units in state  $+1$  can generate force, the normalized force  $f = T_0/T_0^{\max}$  is equal to the average fraction of permissive units:  $f = (1 + \langle s \rangle)/2$ . Taking into account Eqs. (4) and (6), this normalized force can be rewritten as

$$f = \frac{1}{2} \left\{ 1 + \frac{c - 1}{[(c - 1)^2 + 4 n_H^{-2} c]^{1/2}} \right\}. \quad (7)$$

As expected, the above expression is compatible with the tension reaching half of its maximal value at  $c = 1$ , i.e.,  $[\text{Ca}^{2+}] = [\text{Ca}^{2+}]_{50}$ , which justifies the expression of  $c$  introduced in (4).

In both the conventional Hill model (1) and the two state model (7), the Hill coefficient can be recovered using

$$n_H = \frac{d}{d \log c} \log \left( \frac{f}{1 - f} \right) \Big|_{c=1}. \quad (8)$$

Furthermore, in the limits  $c \rightarrow 0$  and  $c \rightarrow \infty$ , the function  $\log_{10}[f/(1 - f)]$  depends linearly on  $\text{pCa} = -\log_{10}([\text{Ca}^{2+}])$  with slope 1 in both cases. Hence, the model can be fully calibrated using the measured value of  $\log_{10}[f/(1 - f)]$  in the region near  $c = 1$ , where this function can be reasonably approximated by a straight line parametrized by the reference concentration  $[\text{Ca}^{2+}]_{50}$  and the slope  $n_H$ .

The calibration is illustrated in Fig. 2, where the force-pCa relation predicted by our model is compared to experimental data obtained from demembrated fibers of rabbit soleus muscle at 25 °C, see [19, 42]. To normalize our experimental data, we used as the reference tension the average force measured at  $\text{pCa} = 4.5$  (saturating concentration) and  $[\text{Ca}^{2+}]_{50} = 10^{-6.5} \text{M}$  as our reference concentration. The value of  $n_H$  was then estimated from the subset of data shown in the inset of Fig. 2(b), using both a custom implementation of the minimum least squared error methods and the built-in non-linear fitting method from Mathematica [43], both giving similar results. We obtained  $n_H = 3.14$  or, equivalently,  $J = 0.57$  according to Eqs. (4).

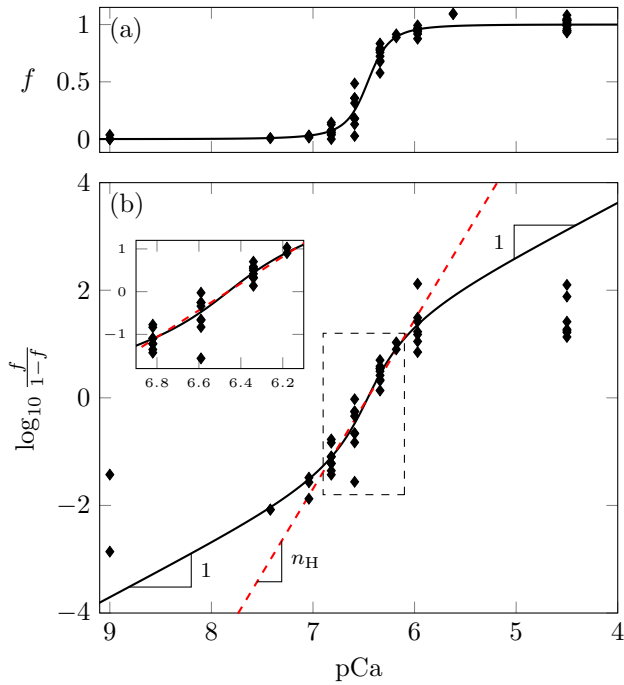


Figure 2. pCa-dependence of the normalized force  $f$  in panel (a) and  $\log_{10}\left(\frac{f}{1-f}\right)$  in panel (b) (black continuous line) obtained after calibration of the model to experimental data (symbols) measured at 25 °C. The experimental data are normalized by the average tension measured at pCa = 4.5. The insert in (b) shows the data chosen to fit the parameter  $n_H$  using linearization at  $c = 1$ , so that the results are not affected by the deviation of the data from the prediction at the extremes of the interval. The best fit [red dashed line in (b)] is achieved setting  $[\text{Ca}^{2+}]_{50} = 10^{-6.5}$  M and  $n_H = 3.14$ . For one fiber, the value of the force at pCa = 9 was measured twice. For that fiber, the mean of the two values was subtracted from the force to all data points generating a negative and a positive value of the same amplitude at pCa 9.

The calibration procedure was repeated on similar data from [19] at 12 °C, 17 °C, 25 °C and 35 °C, and also in the presence of 1  $\mu\text{M}$  OM. It is worth stressing that, for each set of force-pCa curves, the free parameters whose value we fitted are the coupling constant  $J$  and the  $[\text{Ca}^{2+}]_{50}$ . Interestingly, the values of  $[\text{Ca}^{2+}]_{50}$  resulting from the fits do not vary much with temperature.

The fitted values of  $J$  and of the Hill coefficients are represented in Fig. 3 against the force per motor  $F_0$ . The value of  $F_0$  is determined from experiments using the expression  $F_0 = \kappa_0 x_0$ , where  $\kappa_0$  and  $x_0$  denote the stiffness and elongation of a single motor, respectively. Both  $\kappa_0$  and  $x_0$  can be estimated by means of specific mechanical protocols by which the contribution of myosin motors and myofilaments to the half sarcomere compliance during active isometric contraction can be identified [19]. An important experimental finding is that  $F_0$  is independent of  $[\text{Ca}^{2+}]$ , while  $T_0$  increases with  $[\text{Ca}^{2+}]$  in proportion with the number of attached motors  $N_0$ :  $T_0 = N_0 F_0$  [19, 44]. Hence, at each temperature,  $F_0$  can be considered as a

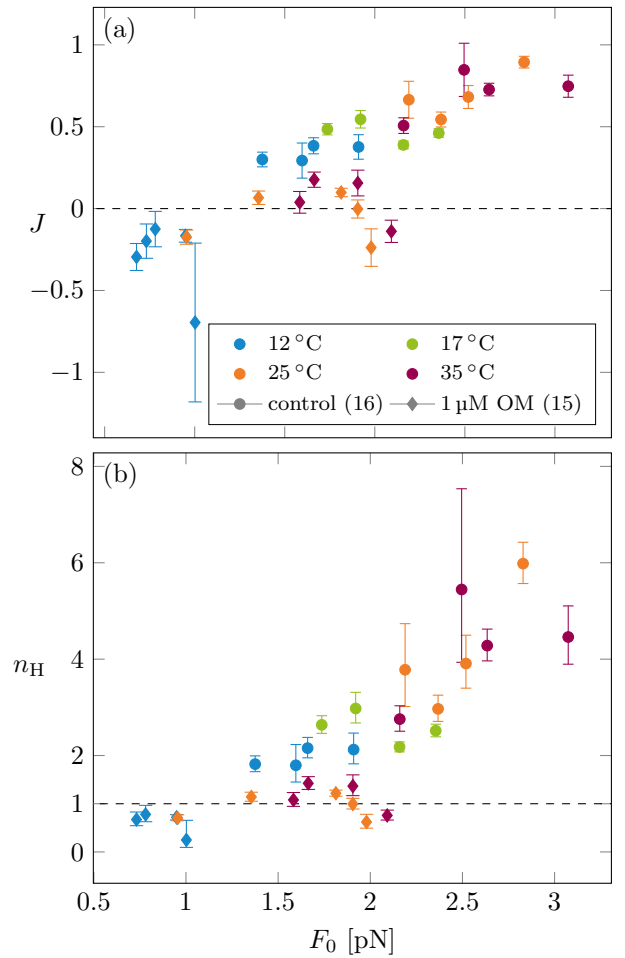


Figure 3. Dependence of the coupling constant  $J$  (a) and of the Hill coefficient  $n_H$  (b) on the motor force modulated by temperature without OM (circles) and in the presence of 1  $\mu\text{M}$  OM (diamonds). Each symbol represents measurement from a single muscle fiber [42]. The results are shown as function of the force per motor  $F_0$  measured for different fibers. Experimental data are taken from [19]. Error bars indicate the error in the calibration. In total, fifteen and sixteen measurements were performed with and without OM, respectively. The number of fibers used for each temperature are indicated in parentheses in the legend.

parameter modulating the cooperativity of the system i.e., how fast  $N_0$  increases with  $[\text{Ca}^{2+}]$ .

For fibers without OM (control), the Hill coefficient almost triples as temperature ranges from 17 °C to 35 °C, signaling a significant increase in cooperativity, see Fig. 3. The obtained values of  $J$  and  $n_H$  are similar between 25 °C and 35 °C. Conversely, in the presence of OM (diamonds), the Hill coefficient takes values smaller than 1 for the temperatures 12 °C, 25 °C and 35 °C. Hence, the presence of OM seems to suppress the cooperative activation. In fact, values of  $n_H$  smaller than 1 implies that  $J < 0$ . Therefore, the interaction term in the one-spin Ising model becomes anti-ferromagnetic. It entails that the presence of a force generating unit disfavors a nearby

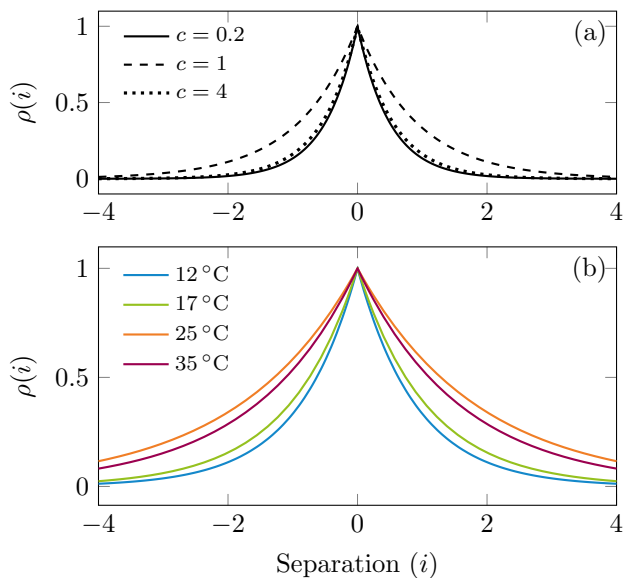


Figure 4. (a) Correlation function at different calcium concentrations obtained from the model fitted to the experimental data at 12 °C. (b) Correlation function at  $c = 1$  for the temperatures 12 °C, 17 °C, 25 °C and 35 °C presented in Fig. 3 in control conditions.

one, so that the system becomes anti-cooperative in this regime.

These findings support the description of the cooperative mechanism put forward in [19], according to which the force generated by an attached motor modulates the probability of activating neighboring RUs, thereby the Hill coefficient.

### B. Correlation between neighboring units

To further characterize the cooperative mechanism, we introduce the correlation function

$$\rho(i) := \frac{\langle s_0 s_i \rangle - \langle s \rangle^2}{\langle s_0^2 \rangle - \langle s \rangle^2}, \quad (9)$$

which quantifies the tendency for a remote site  $i$  to be in the same configuration as an arbitrary reference site 0. For the sake of simplicity, we discuss only the case of  $J \geq 0$  (i.e.,  $n_H \geq 1$ ) for which we have  $\rho(i) = (\lambda_-/\lambda_+)^i$ , where  $\lambda_{\pm} = e^J \{ \cosh(h) \pm [\sinh^2(h) + e^{-4J}]^{1/2} \}$  are the eigenvalues of the transfer matrix [45].

The spreading of the correlation function is maximum at  $c = 1$ , see Fig. 4(a), coherently with the fact that this concentration also correspond to the highest slope of the force-pCa curve, see Fig. 2(a). Furthermore, the correlation length increases with the force per motor, as expected from the increase in the cooperativity, see Fig. 4(b). At low forces (temperature 12 °C), the influence of the single unit is negligibly small beyond the

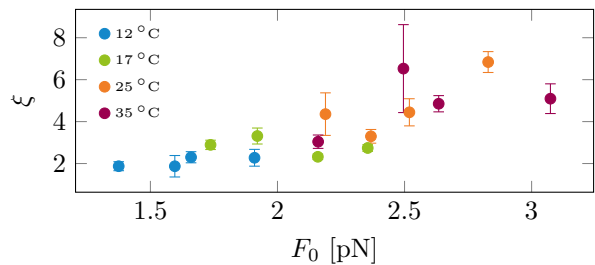


Figure 5. Correlation length  $\xi$  as a function of the force per motor  $F_0$  modulated by temperature.

fourth neighbor, while it largely exceeds this range at higher forces (temperatures  $> 25$  °C).

The dependence of the cooperative mechanism on the force per motor can be characterized by the correlation length [45, 46]  $\xi = [\log(\lambda_+/\lambda_-)]^{-1}$ , which reads as

$$\xi = \left[ \log \left( \frac{n_H + 1}{n_H - 1} \right) \right]^{-1} \quad (10)$$

when  $c = 1$ . As for the Hill coefficient (see Fig. 3), we obtain an increase of the correlation length  $\xi$  with the increase of the force per motor  $F_0$ , from  $\xi \approx 2$  at 12 °C to  $\xi \approx 6$  at 25 °C and 35 °C in control conditions, see Fig. 5.

Overall, the above analysis of the correlations between neighboring of the single (two-state) spin model in the presence or absence of OM tends to support the hypothesis that spreading of the activation signal to neighboring RUs is due to the increase of motor force at submaximal calcium concentration.

## III. COMPARISON WITH A FOUR-STATE MODEL

As mentioned in the Introduction, a description for the activation of units generating force was proposed by Rice et al. [37], introducing a model of spins structured in two layers. Below, after briefly reviewing their approach, we reformulate it in terms of a generalized external field that allows for a simpler interpretation of the output force and a comparison with our model.

### A. Original formulation

The system in [37] is represented as a chain of  $N$  units, each being characterized by two spins:  $\sigma = \pm 1$  and  $\delta = \pm 1$ . The spin  $\delta$  takes the value  $+1$  when a  $\text{Ca}^{2+}$  is bound, and the value  $-1$  if not. The spin  $\sigma$ , instead, takes the value  $+1$  if a myosin head can attach and generate force (i.e., the unit is permissive), and the value  $-1$  if the myosin head cannot attach (i.e., the unit is non-permissive). Together,  $\delta$  and  $\sigma$  define four states ( $\begin{smallmatrix} \delta \\ \sigma \end{smallmatrix}$ ) schematized in Fig. 6. The configuration of the whole

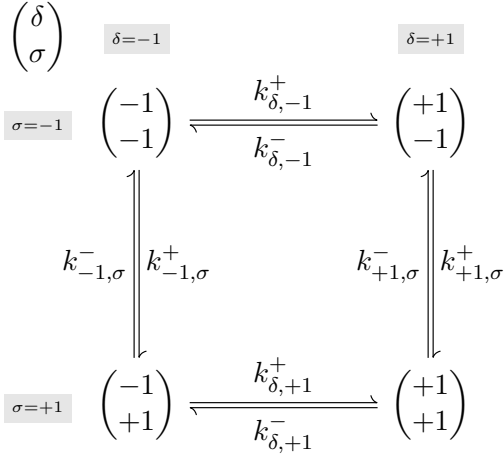


Figure 6. Four-state model proposed by Rice et al. [37]. The system consists of a 1D chain of  $N$  units, each being described with two spins  $\sigma = \pm 1$  and  $\delta = \pm 1$  generating four possible states. The transitions between the different states are characterized by the set of rate constants  $k_{\delta,\sigma}^{\pm}$ .

system is then characterized by the set of spins of all units  $\{(\delta_i, \sigma_i), i \in \{1, \dots, N\}\}$ , which, for an actin filament constituted of 26 regulatory units, represents  $4^{26}$  distinct configurations.

The dimensionless Hamiltonian of this two-spin system can be written as [37]

$$H_2 = - \sum_{i=1}^N (J\sigma_i\sigma_{i+1} + K\sigma_i\delta_i + h_\delta\delta_i + h_\sigma\sigma_i), \quad (11)$$

where  $h_\delta$  and  $h_\sigma$  play the role of external fields associated with the spins  $\delta_i$  and  $\sigma_i$ , respectively. The parameter  $K$  is a coupling for spins of different species on site  $i$ , and  $J$  accounts for nearest-neighbor interactions for spins  $\sigma_i$ . The associated jump process is characterized by eight transition rates  $k_{\delta,\sigma}^{\pm}$ , see Fig. 6. For instance, the rate  $k_{-1,\sigma}^+$  (respectively  $k_{-1,\sigma}^-$ ) is associated with the transition from the state  $\begin{pmatrix} -1 \\ -1 \end{pmatrix}$  (respectively,  $\begin{pmatrix} -1 \\ +1 \end{pmatrix}$ ) to state  $\begin{pmatrix} -1 \\ +1 \end{pmatrix}$  (respectively,  $\begin{pmatrix} -1 \\ -1 \end{pmatrix}$ ), see Fig. 6.

As shown in Ref. [37], the equilibrium response of the system can be described in terms of the parameters  $C$ ,  $Q$ ,  $\mu$ , and  $\gamma$  defined by

$$\begin{aligned} \frac{1}{2} \log(C) &= h_\delta - K, & \frac{1}{2} \log(Q) &= h_\sigma + K, \\ \frac{1}{4} \log(\mu) &= K, & \frac{1}{2} \log(\gamma) &= J. \end{aligned}$$

The average normalized force produced by the system is given by the fraction of units in the permissive state:  $f = (1 + \langle \sigma \rangle)/2$ , which thus combine the populations in states  $\begin{pmatrix} -1 \\ +1 \end{pmatrix}$  and  $\begin{pmatrix} +1 \\ +1 \end{pmatrix}$ . In particular, taking the large  $N$

limit, the average normalized force takes the form [37]

$$f = \frac{1}{2} \left\{ 1 + \frac{AC + B}{[(AC + B)^2 + 4D(C + 1)(\mu C + 1)]^{1/2}} \right\}, \quad (12)$$

where

$$\begin{aligned} A &= \mu^{1/4} (Q^{1/2} - Q^{-1/2}), \\ B &= \mu^{-3/4} (Q^{1/2} - \mu Q^{-1/2}), \\ D &= \gamma^{-2} \mu^{-1/2}. \end{aligned}$$

## B. Reformulation

Here, we choose a different parametrization of the previous four-state model by introducing the following quantities:

$$\frac{1}{2} \log(c) = h_\sigma + h_\delta, \quad \frac{1}{2} \log(p) = h_\sigma - K, \quad (13a)$$

$$\frac{1}{2} \log(q) = h_\delta - K, \quad \frac{1}{2} \log(n_H) = J. \quad (13b)$$

With this new set of parameters, the force (12) can now be written (see Appendix A) as

$$f = \frac{1}{2} \left\{ 1 + \frac{x - 1}{[(x - 1)^2 + 4n_H^{-2}x]^{1/2}} \right\}, \quad (14)$$

which is analogous to (7) using the equivalent external field

$$x = \frac{c + p}{q + 1}. \quad (15)$$

This result shows that, like in the two state Ising model, the force is determined by only two independent parameters, namely  $x$  and  $n_H$ . Hence, the data of the force-pCa relation alone cannot fully determine the four-state model.

## C. Detailed balance conditions and calcium dependence

Using the mapping (13), we can write the detailed balance conditions associated with the different transition rates represented in Fig. 6 (see Appendix B) as

$$\frac{k_{\delta,-1}^+}{k_{\delta,-1}^-} = q, \quad \frac{k_{\delta,+1}^+}{k_{\delta,+1}^-} = \frac{c}{p}, \quad (16a)$$

$$\frac{k_{-1,\sigma}^+}{k_{-1,\sigma}^-} = p n_H^{(\sigma_{i-1} + \sigma_{i+1})}, \quad \frac{k_{+1,\sigma}^+}{k_{+1,\sigma}^-} = \frac{c}{q} n_H^{(\sigma_{i-1} + \sigma_{i+1})}. \quad (16b)$$

To compare the model (11) with experimental data, Rice et al. consider that the concentration in calcium ions affects only the kinetics of the transition  $\delta_i = -1 \rightarrow \delta_i =$

+1, which means in our case that  $p$  is independent on  $[\text{Ca}^{2+}]$ . Assuming first order kinetics, Rice et al. considered  $q = \frac{k_{\delta,-1}^+}{k_{\delta,-1}^-} = \frac{[\text{Ca}^{2+}]}{K_d}$ , where  $K_d$  is the calcium dissociation constant in the non-permissive states. Similarly,  $\frac{c}{p} = \frac{k_{\delta,+1}^+}{k_{\delta,+1}^-} = \frac{[\text{Ca}^{2+}]}{K'_d}$  (if  $p \neq 0$ ), where  $K'_d$  is the calcium dissociation constant in the permissive states. These hypotheses reveal the dependence of our effective field  $x$  on  $[\text{Ca}^{2+}]$  (provided  $p \neq 0$ ):

$$x = \frac{K_d}{pK'_d} \frac{([\text{Ca}^{2+}] + K'_d)}{([\text{Ca}^{2+}] + K_d)}. \quad (17)$$

We first notice that in the particular case where  $K_d = K'_d$ , we have  $x = 1/p$ , which is independent on  $[\text{Ca}^{2+}]$ . Second, when  $[\text{Ca}^{2+}] \rightarrow \infty$ ,  $x \rightarrow \frac{K_d}{pK'_d}$ , which implies that the system does not necessarily reach the maximum tension  $f = 1$  even at large  $[\text{Ca}^{2+}]$ . Third, when  $[\text{Ca}^{2+}] \rightarrow 0$ ,  $x \rightarrow \frac{1}{p}$ , which implies that the system might generate force even without calcium. Interestingly, the system may reach  $f = 1$  at saturating calcium if  $p \rightarrow 0$ , which can be achieved if  $h_\sigma \rightarrow -\infty$ . Conversely, the system can reach  $f = 0$  at low calcium concentration if  $p \rightarrow \infty$ , obtained if  $h_\sigma \rightarrow +\infty$ . Otherwise, for other values of  $h_\sigma$ , the correct limits at low and high calcium concentrations are not correctly reproduced by the model.

#### D. Reduced two-state models

We now study how the generated force depends on the coupling  $K$  between the two spins of the Rice et al. model. First, we consider complete uncoupling by setting  $K = 0$ . In such a case, we have  $x = p = \exp[2h_\sigma]$ , which means that the effective field is the one associated with the spin  $\sigma$ , see (11). In particular, in this limit, the force becomes independent of  $[\text{Ca}^{2+}]$ .

Second, we now consider the strong coupling limit  $K \rightarrow \infty$ , which implies  $p \rightarrow 0$  and  $q \rightarrow 0$  so that  $x = c = \exp[2(h_\sigma + h_\delta)]$ . Recalling the detailed balance relations (16), the limits  $p \rightarrow 0$  and  $q \rightarrow 0$  imply that the heterogeneous states  $\begin{pmatrix} -1 \\ +1 \end{pmatrix}$  and  $\begin{pmatrix} +1 \\ -1 \end{pmatrix}$  (bottom left and top right corners in Fig. 6) will not be populated, leaving only the homogeneous states  $\begin{pmatrix} -1 \\ -1 \end{pmatrix}$  and  $\begin{pmatrix} +1 \\ +1 \end{pmatrix}$ . This result can also be inferred from the Hamiltonian (11) since high values of  $K$  will favor the homogeneous states. Therefore, the strong coupling limit leads to a single spin model with  $s_i = \begin{pmatrix} -1 \\ -1 \end{pmatrix}$  or  $s_i = \begin{pmatrix} +1 \\ +1 \end{pmatrix}$ , whose response does depend on calcium concentration, and which is then fully analog to the one-spin (two-state) model presented in Section II.

To support this statement, we compute the equilibrium constant of the two reaction paths  $[\begin{pmatrix} -1 \\ -1 \end{pmatrix} \rightarrow \begin{pmatrix} +1 \\ +1 \end{pmatrix}] \rightarrow [\begin{pmatrix} +1 \\ -1 \end{pmatrix}]$  and  $[\begin{pmatrix} -1 \\ -1 \end{pmatrix} \rightarrow \begin{pmatrix} -1 \\ +1 \end{pmatrix}] \rightarrow [\begin{pmatrix} +1 \\ +1 \end{pmatrix}]$ . For both paths we find:

$$\frac{[\begin{pmatrix} +1 \\ +1 \end{pmatrix}]}{[\begin{pmatrix} -1 \\ -1 \end{pmatrix}]} = \frac{k_{\delta,-1}^+ k_{+1,\sigma}^+}{k_{\delta,-1}^- k_{+1,\sigma}^-} = \frac{k_{-1,\sigma}^+ k_{\delta,+1}^+}{k_{-1,\sigma}^- k_{\delta,+1}^-} = c n_H^{(s_{i-1} + s_{i+1})} \quad (18)$$

that corresponds to the detailed balance (5) under the combined field  $h_\sigma + h_\delta$  and the identification of the coupled spins  $\begin{pmatrix} \delta_i \\ \sigma_i \end{pmatrix}$  with  $s_i$ . Notice that Eq. (18) is valid also when  $K$  is finite, meaning that the only field that controls the ratio of populations in states  $\begin{pmatrix} -1 \\ -1 \end{pmatrix}$  and  $\begin{pmatrix} +1 \\ +1 \end{pmatrix}$  is  $h_\sigma + h_\delta$ , independently on the coupling between the spins.

## IV. DISCUSSION

### A. Alternative models

This work presents a model of the thin filament activation for muscle contraction based on a single spin (two-state) Ising model where a unit can be either “non-force-generating” or “force-generating”. The model incorporates two key parameters: a control parameter  $h$  linked to the experimental calcium concentration, and a free parameter  $J$  that determines the energy gain resulting from having two consecutive units in the same state. Therefore,  $J$  quantifies cooperativity. These phenomenological parameters are not directly related to the actual molecular mechanisms at work during activation; they are introduced to effectively reproduce the behavior observed in experimental data, as customary for such systems.

In terms of complexity, our two-state Ising model has direct correspondence with the classical Hill model, which also relies on two parameters: the reference concentration  $[\text{Ca}^{2+}]_{50}$  and the Hill coefficient  $n_H$ . The advantage of the Ising model lies in its ability to provide a mechanistic interpretation of the Hill coefficient in terms of nearest-neighbor interactions. It also allows for the computation of correlation functions and correlation lengths, which are not accessible through the Hill model.

After normalization of  $h$  using the reference calcium concentration  $[\text{Ca}^{2+}]_{50}$  that is directly obtained from experiments, the behavior of our model is fully determined by the sole coupling constant  $J$ . We have thus showed that the resulting one-parameter model is sufficient to accurately reproduce the experimental force-pCa curves.

More detailed representations of thin filament activation have been proposed in the literature, often implementing the so-called “blocked-closed-open” paradigm introduced by McKillop and Geeves [16]. The corresponding models are usually built upon Huxley-Hill type framework for modeling unregulated actin-myosin interactions [26]. Huxley-Hill type models capture time-dependent behaviors and can be calibrated using a large variety of experimental observations ranging from single molecule experiments to in-vitro motility assays and fiber mechanics. The cooperative filament activation can then be accounted for by ad-hoc variations of the attachment rate of unbound motors with the distance from already attached motors [18, 24, 47, 48]. Once the parameters of underlying actin-myosin interaction model are calibrated using data obtained at saturating  $[\text{Ca}^{2+}]$ , the modulation

of actin-myosin interactions is then adjusted to match data obtained by varying  $[\text{Ca}^{2+}]$ . This modulation can effectively rely on few additional parameters.

In all cases, these formulations involve defining rate functions that may be associated with a virtually infinite number of parameters. These rate functions can eventually be parametrized by few scalars that nevertheless necessitate more experimental data than the sole force-pCa curves considered in the present work to be specifically identified.

Furthermore, in the framework of Ising-like models, accounting for the blocked-closed-open paradigm requires at least two spin variables, as proposed by Rice et al. [37], but we here demonstrate that such four state model can be mapped into a simpler two state version for the fitting of force-pCa relation.

In summary, the model used in this paper can be viewed as a drastically reduced version of these more comprehensive approaches where we assume that both activation states and actin-myosin interaction states can be lumped in two effective states, and that the dynamics of transitions between these states can be neglected in favor of an equilibrium description for the steady state force-pCa curves.

## B. Cooperativity

Despite its simplicity, our approach successfully captures the characteristic features of the force-pCa curve, including the upper and lower limits, and its sigmoidal shape. The model leverages nearest-neighbor interactions within the Ising framework to elucidate how cooperativity operates at the filament level. The coupling coefficient  $J$  quantifies the energy required, in units of  $k_B T$ , to match the observed effect of temperature changes on the degree of cooperativity illustrated by variation in both the Hill coefficient and the correlation length between neighboring regulatory units. The increased correlation length can be interpreted as a stronger head-tail molecular interaction between consecutive tropomyosin proteins along the actin filament [49–51].

## C. Effect of omecamtiv mecarbil

Our analysis reveals distinct behaviors for fibers in control conditions and fibers treated with OM. Notably, the cooperativity parameter becomes negative in the presence of OM, suggesting that the drug not only disrupts cooperativity but can also introduce anti-cooperativity within the thin filament. In the present context, anti-cooperativity is defined by a Hill coefficient  $n_H < 1$  following the terminology used for protein-ligand binding systems, or equivalently a negative coupling constant  $J < 0$  as in antiferromagnetic systems.

This finding aligns with the experimental observations at 12 °C from Refs. [19, 25], reporting values of  $n_H =$

$0.79 \pm 0.09$  and  $n_H = 0.84 \pm 0.15$ , respectively. At room temperature, the effect of OM is less pronounced with observed values down to  $n_H \approx 1$  [19, 23, 25], though a value slightly below 1 ( $0.97 \pm 0.07$ ) is reported for rat cardiomyocytes in Ref. [23].

The effect of OM on force generation by actin-myosin system has been studied at the molecular level by Woody et al. [24] based on the model developed in [18, 47, 48]. The experimental data obtained by Woody et al. on single molecules can then be reproduced by modulating the kinetics of the actin-myosin interaction, particularly by reducing the detachment rate of OM-bound myosin heads and the power-stroke size. They show that this modulation can account for the effect of OM on calcium sensitivity, materialized by horizontal shifts of the force-pCa curve. However, the effect of OM on cooperativity, as measured by the Hill coefficient is not explicitly addressed.

The results obtained by Caremani et al. [19] and Governali et al. [25] suggest that variation in the Hill coefficient with OM cannot be explained solely by the reduction of the force per motor induced by OM binding, and therefore that OM would not affect only single motor properties as postulated by Woody et al. Hence, their result support the hypothesis that OM indirectly modulates the interaction between neighboring units, which is precisely what we quantify through variation of the coupling constant with OM.

## D. Limitations

A potential limitation of this work is that it is based on an approach that is valid under thermodynamic equilibrium conditions. Physiologically, muscle consumes energy even during isometric contraction, where no mechanical work is performed, which implies that the system breaks the detailed balance condition [52, 53]. Nevertheless, in this work we implicitly assume that effective free energy landscapes can be defined, an approximation that is also guided by the fact that no external action is exerted on the system once steady state is reached.

The next step in our research involves establishing a quantitative relationship between thin filament cooperativity and the availability of myosin motor from the nearby thick filaments with the aim to achieve a deeper understanding of the interplay between thin filament cooperativity and thick filament regulation [11, 54, 55]. The predictions of the model should also be tested using experimental data from different muscle types and species, and in different experimental conditions to assess its generality.

## ACKNOWLEDGMENTS

We thank Vincenzo Lombardi and Massimo Reconditi for continuous discussion and critical reading of

the manuscript. I.L. acknowledges financial support from the Spanish Government through grants PID2021-126570NB-I00 and PID2024-156516NB-I00 financed by MICIU/AEI/10.13039/501100011033 and FEDER/UE. S.G., S.R. and M.L. acknowledges financial support from

the European Union — NextGeneration EU within PRIN 2022, PNRR M4C2, Project P2022XPT32 Regulation of striated muscle: a research bridging single molecule to organ (ResTriMus) [CUP B53D23033290001]

### Appendix A: Effective field

We now discuss the mathematical steps to obtain Eq. (14). For this purpose, it is convenient to express the normalized force in terms of the parameters of the Hamiltonian (11) of the two-spin system. The direct application of the transfer matrix method entails the following expression:

$$f = \frac{1}{2} \left( 1 + \frac{e^{h_\sigma+2h_\delta} + e^{h_\sigma-2K} - e^{2h_\delta-h_\sigma-2K} - e^{-h_\sigma}}{\left( (e^{h_\sigma+2h_\delta} + e^{h_\sigma-2K} - e^{2h_\delta-h_\sigma-2K} - e^{-h_\sigma})^2 + 4e^{-4J} (e^{4h_\delta-2K} + e^{2h_\delta-4K} + e^{2h_\delta} + e^{-2K}) \right)^{1/2}} \right).$$

Thus, factorizing the numerator and the denominator by  $\exp(-h_\sigma)$  and using the definitions (13) leads us straightforwardly to (14) with the effective field  $x = \frac{c+p}{q+1}$ .

### Appendix B: Detailed balance relation

In this Appendix we report the rationale that entails the detailed balance conditions associated with the transition rates represented in Fig. 6. Denoting  $\sigma_{i\pm 1} = \sigma_{i-1} + \sigma_{i+1}$ , equations (16) are obtained by explicitly writing the identities

$$\begin{aligned} \frac{k_{\delta,j}^+}{k_{\delta,j}^-} &= \exp(-H_2(\delta_i = +1, \sigma_i = j) + H_2(\delta_i = -1, \sigma_i = j)), \\ \frac{k_{j,\sigma}^+}{k_{j,\sigma}^-} &= \exp(-H_2(\delta_i = j, \sigma_i = +1) + H_2(\delta_i = j, \sigma_i = -1)), \end{aligned}$$

with  $j \in \{+1, -1\}$ , namely

$$\begin{aligned} \frac{k_{\delta,-1}^+}{k_{\delta,-1}^-} &= \exp(-(K(-1)(-1) - h_\delta) + (K(+1)(-1) + h_\delta)) = \exp(2(h_\delta - K)) = q, \\ \frac{k_{\delta,+1}^+}{k_{\delta,+1}^-} &= \exp(-(K(-1)(+1) - h_\delta) + (K(+1)(+1) + h_\delta)) = \exp(2(h_\delta + K)) = \frac{\exp(2(h_\delta + h_\sigma))}{\exp(2(h_\sigma - K))} = \frac{c}{p}, \\ \frac{k_{-1,\sigma}^+}{k_{-1,\sigma}^-} &= \exp(-J(\sigma_{i\pm 1})(-1) - K(-1)(-1) - h_\sigma(-1) + J(\sigma_{i\pm 1}) + K(-1)(+1) + h_\sigma) = \\ &= \exp(2J\sigma_{i\pm 1}) \exp(2h_\sigma - 2K) = p n_{\text{H}}^{\sigma_{i\pm 1}}, \\ \frac{k_{+1,\sigma}^+}{k_{+1,\sigma}^-} &= \exp(-J(\sigma_{i\pm 1})(+1) - K(+1)(-1) - h_\sigma(-1) + J(\sigma_{i\pm 1}) + K(+1)(+1) + h_\sigma) = \\ &= \exp(2J\sigma_{i\pm 1}) \exp(2h_\sigma + 2K) = n_{\text{H}}^{\sigma_{i\pm 1}} \frac{\exp(2(h_\delta + h_\sigma))}{\exp(2(h_\delta - K))} = \frac{c}{q} n_{\text{H}}^{\sigma_{i\pm 1}}. \end{aligned}$$

- 
- [1] H. E. Huxley, Muscle 1972: Progress and Problems, Cold Spring Harbor Symposia on Quantitative Biology **37**, 689 (1973).  
 [2] A. M. Gordon, E. Homsher, and M. Regnier, Regulation of Contraction in Striated Muscle, Physiological Reviews

- 80**, 853 (2000).  
 [3] J. L. Woodhead, F.-Q. Zhao, R. Craig, E. H. Egelman, L. Alamo, and R. Padrón, Atomic model of a myosin filament in the relaxed state, Nature **436**, 1195 (2005).

- [4] M. A. Stewart, K. Franks-Skiba, S. Chen, and R. Cooke, Myosin ATP turnover rate is a mechanism involved in thermogenesis in resting skeletal muscle fibers, *Proceedings of the National Academy of Sciences* **107**, 430 (2010).
- [5] H. E. Huxley, Muscular Contraction and Cell Motility, *Nature* **243**, 445 (1973).
- [6] M. Linari, E. Brunello, M. Reconditi, L. Fusi, M. Caremani, T. Narayanan, G. Piazzesi, V. Lombardi, and M. Irving, Force generation by skeletal muscle is controlled by mechanosensing in myosin filaments, *Nature* **528**, 276 (2015).
- [7] M. Reconditi, M. Caremani, F. Pinzauti, J. D. Powers, T. Narayanan, G. J. M. Stienen, M. Linari, V. Lombardi, and G. Piazzesi, Myosin filament activation in the heart is tuned to the mechanical task, *Proceedings of the National Academy of Sciences* **114**, 3240 (2017).
- [8] G. Piazzesi, M. Caremani, M. Linari, M. Reconditi, and V. Lombardi, Thick Filament Mechano-Sensing in Skeletal and Cardiac Muscles: A Common Mechanism Able to Adapt the Energetic Cost of the Contraction to the Task, *Frontiers in Physiology* **9**, 736 (2018).
- [9] E. Brunello, L. Fusi, A. Ghisleni, S.-J. Park-Holohan, J. G. Ovejero, T. Narayanan, and M. Irving, Myosin filament-based regulation of the dynamics of contraction in heart muscle, *Proceedings of the National Academy of Sciences* **117**, 8177 (2020).
- [10] C. Squarci, P. Bianco, M. Reconditi, I. Pertici, M. Caremani, T. Narayanan, Á. I. Horváth, A. Málnási-Csizmadia, M. Linari, V. Lombardi, and G. Piazzesi, Titin activates myosin filaments in skeletal muscle by switching from an extensible spring to a mechanical rectifier, *Proceedings of the National Academy of Sciences* **120**, e2219346120 (2023).
- [11] I. Morotti, M. Caremani, M. Marcello, I. Pertici, C. Squarci, P. Bianco, T. Narayanan, G. Piazzesi, M. Reconditi, V. Lombardi, and M. Linari, An integrated picture of the structural pathways controlling the heart performance, *Proceedings of the National Academy of Sciences* **121**, e2410893121 (2024).
- [12] A. Weber and J. M. Murray, Molecular control mechanisms in muscle contraction., *Physiological Reviews* **53**, 612 (1973).
- [13] D. R. Swartz and R. L. Moss, Influence of a strong-binding myosin analogue on calcium-sensitive mechanical properties of skinned skeletal muscle fibers., *Journal of Biological Chemistry* **267**, 20497 (1992).
- [14] P. Vibert, R. Craig, and W. Lehman, Steric-model for activation of muscle thin filaments, *Journal of Molecular Biology* **266**, 8 (1997).
- [15] R. Craig and W. Lehman, Crossbridge and tropomyosin positions observed in native, interacting thick and thin filaments, *Journal of Molecular Biology* **311**, 1027 (2001).
- [16] D. McKillop and M. Geeves, Regulation of the interaction between actin and myosin subfragment 1: Evidence for three states of the thin filament, *Biophysical Journal* **65**, 693 (1993).
- [17] R. Desai, M. A. Geeves, and N. M. Kad, Using Fluorescent Myosin to Directly Visualize Cooperative Activation of Thin Filaments, *Journal of Biological Chemistry* **290**, 1915 (2015).
- [18] T. Longyear, S. Walcott, and E. P. Debold, The molecular basis of thin filament activation: From single molecule to muscle, *Scientific Reports* **7**, 1822 (2017).
- [19] M. Caremani, M. Marcello, I. Morotti, I. Pertici, C. Squarci, M. Reconditi, P. Bianco, G. Piazzesi, V. Lombardi, and M. Linari, The force of the myosin motor sets cooperativity in thin filament activation of skeletal muscles, *Communications Biology* **5**, 1 (2022).
- [20] D. G. Moiescu, Kinetics of reaction in calcium-activated skinned muscle fibres, *Nature* **262**, 610 (1976).
- [21] A. V. Hill, The possible effects of the aggregation of the molecules of haemoglobin on its dissociation curves, *The Journal of Physiology* **40**, iv (1910).
- [22] F. I. Malik, J. J. Hartman, K. A. Elias, B. P. Morgan, H. Rodriguez, K. Brejc, R. L. Anderson, S. H. Sueoka, K. H. Lee, J. T. Finer, R. Sakowicz, R. Baliga, D. R. Cox, M. Garard, G. Godinez, R. Kawas, E. Kraynack, D. Lenzi, P. P. Lu, A. Muci, C. Niu, X. Qian, D. W. Pierce, M. Pokrovskii, I. Suehiro, S. Sylvester, T. Tochimoto, C. Valdez, W. Wang, T. Katori, D. A. Kass, Y.-T. Shen, S. F. Vatner, and D. J. Morgans, Cardiac Myosin Activation: A Potential Therapeutic Approach for Systolic Heart Failure, *Science* **331**, 1439 (2011).
- [23] L. Nagy, Á. Kovács, B. Bódi, E. T. Pásztor, G. Á. Fülöp, A. Tóth, I. Édes, and Z. Papp, The novel cardiac myosin activator omecamtiv mecarbil increases the calcium sensitivity of force production in isolated cardiomyocytes and skeletal muscle fibres of the rat, *British Journal of Pharmacology* **172**, 4506 (2015).
- [24] M. S. Woody, M. J. Greenberg, B. Barua, D. A. Winkelmann, Y. E. Goldman, and E. M. Ostap, Positive cardiac inotrope omecamtiv mecarbil activates muscle despite suppressing the myosin working stroke, *Nature Communications* **9**, 3838 (2018).
- [25] S. Governali, M. Caremani, C. Gallart, I. Pertici, G. Stienen, G. Piazzesi, C. Ottenheijm, V. Lombardi, and M. Linari, Orthophosphate increases the efficiency of slow muscle-myosin isoform in the presence of omecamtiv mecarbil, *Nature Communications* **11**, 3405 (2020).
- [26] T. L. Hill, Theoretical formalism for the sliding filament model of contraction of striated muscle Part I, *Progress in Biophysics and Molecular Biology* **28**, 267 (1974).
- [27] T. L. Hill, Theoretical formalism for the sliding filament model of contraction of striated muscle part II, *Progress in Biophysics and Molecular Biology* **29**, 105 (1976).
- [28] S. M. Mijailovich, O. Kayser-Herold, X. Li, H. Griffiths, and M. A. Geeves, Cooperative regulation of myosin-S1 binding to actin filaments by a continuous flexible Tm-Tn chain, *European Biophysics Journal* **41**, 1015 (2012).
- [29] D. A. Smith and S. M. Mijailovich, Toward a Unified Theory of Muscle Contraction. II: Predictions with the Mean-Field Approximation, *Annals of Biomedical Engineering* **36**, 1353 (2008-08).
- [30] D. Smith, M. Geeves, J. Sleep, and S. Mijailovich, Towards a Unified Theory of Muscle Contraction. I: Foundations, *Annals of Biomedical Engineering* **36**, 1624 (2008-10).
- [31] M. Caremani, L. Melli, M. Dolfi, V. Lombardi, and M. Linari, The working stroke of the myosin II motor in muscle is not tightly coupled to release of orthophosphate from its active site, *The Journal of Physiology* **591**, 5187 (2013-10-15).
- [32] S. M. Mijailovich, M. Prodanovic, C. Poggesi, M. A. Geeves, and M. Regnier, Multiscale modeling of twitch contractions in cardiac trabeculae, *Journal of General*

- Physiology **153**, e202012604 (2021).
- [33] B. Stojanovic, M. Svicevic, A. Kaplarevic-Malisic, R. J. Gilbert, and S. M. Mijailovich, Multi-scale Striated Muscle Contraction Model Linking Sarcomere Length-dependent Cross-bridge Kinetics to Macroscopic Deformation, *Journal of Computational Science*, 101062 (2019).
- [34] T. Liu, X. Li, Y. Wang, M. Zhou, and F. Liang, Computational modeling of electromechanical coupling in human cardiomyocyte applied to study hypertrophic cardiomyopathy and its drug response, *Computer Methods and Programs in Biomedicine* **231**, 107372 (2023-04).
- [35] F. Regazzoni, L. Dedè, and A. Quarteroni, Biophysically detailed mathematical models of multiscale cardiac active mechanics, *PLOS Computational Biology* **16**, e1008294 (2020).
- [36] N. Filipovic, T. Sustersic, M. Milosevic, B. Milicevic, V. Simic, M. Prodanovic, S. Mijailovic, and M. Kojic, SILICOFCM platform, multiscale modeling of left ventricle from echocardiographic images and drug influence for cardiomyopathy disease, *Computer Methods and Programs in Biomedicine* **227**, 107194 (2022-12-01).
- [37] J. J. Rice, G. Stolovitzky, Y. Tu, and P. P. de Tombe, Ising Model of Cardiac Thin Filament Activation with Nearest-Neighbor Cooperative Interactions, *Biophysical Journal* **84**, 897 (2003).
- [38] M. Regnier, A. J. Rivera, C.-K. Wang, M. A. Bates, P. B. Chase, and A. M. Gordon, Thin filament near-neighbour regulatory unit interactions affect rabbit skeletal muscle steady-state force-Ca<sup>2+</sup> relations, *The Journal of Physiology* **540**, 485 (2002).
- [39] R. Zwanzig, Nonequilibrium statistical mechanics, in *Nonequilibrium Statistical Mechanics* (Oxford: Oxford University Press), 2001 Chap. 4.
- [40] R. Livi and P. Politi, *Nonequilibrium Statistical Physics: A Modern Perspective*, 1st ed. (Cambridge University Press, 2017).
- [41] Interested readers can refer for instance to pp. 204-210 of Baxter's book [45] or to [46, 56].
- [42] M. Caremani and M. Linari, <https://doi.org/10.5281/ZENODO.18735637> Force-pca relations from rabbit psoas at different temperatures and in presence of omecamtiv mevarbil (2026).
- [43] W. Research, Nonlinearmodelfit, <https://reference.wolfram.com/language/ref/NonlinearModelFit.html> (2025), [Accessed: 16-August-2025].
- [44] M. Linari, M. Caremani, C. Piperio, P. Brandt, and V. Lombardi, Stiffness and Fraction of Myosin Motors Responsible for Active Force in Permeabilized Muscle Fibers from Rabbit Psoas, *Biophysical Journal* **92**, 15 (2007).
- [45] R. Baxter, Exactly solved models in statistical mechanics, in *Exactly Solved Models in Statistical Mechanics* (Elsevier Science & Technology, 2016) Chap. 2, pp. 35–37.
- [46] H. Nishimori and G. Ortiz, Elements of phase transitions and critical phenomena, in *Elements of Phase Transitions and Critical Phenomena* (Oxford University Press, 2011) pp. 204–210.
- [47] S. Walcott, Muscle activation described with a differential equation model for large ensembles of locally coupled molecular motors, *Physical Review E* **90**, 042717 (2014).
- [48] E. P. Debold, S. Walcott, M. Woodward, and M. A. Turner, Direct Observation of Phosphate Inhibiting the Force-Generating Capacity of a Miniensemble of Myosin Molecules, *Biophysical Journal* **105**, 2374 (2013).
- [49] C. M. Risi, B. Belknap, J. Atherton, I. L. Coscarella, H. D. White, P. Bryant Chase, J. R. Pinto, and V. E. Galkin, Troponin Structural Dynamics in the Native Cardiac Thin Filament Revealed by Cryo Electron Microscopy, *Journal of Molecular Biology* **436**, 168498 (2024-03-15).
- [50] C. M. Risi, B. Belknap, H. D. White, K. Dryden, J. R. Pinto, P. B. Chase, and V. E. Galkin, High-resolution cryo-EM structure of the junction region of the native cardiac thin filament in relaxed state, *PNAS Nexus* **2**, pgac298 (2023-01-10).
- [51] Y. Yamada, K. Namba, and T. Fujii, Cardiac muscle thin filament structures reveal calcium regulatory mechanism, *Nature Communications* **11**, 153 (2020-01-09).
- [52] F. Jülicher, A. Ajdari, and J. Prost, Modeling molecular motors, *Reviews of Modern Physics* **69**, 1269 (1997).
- [53] H. Wang and G. Oster, Ratchets, power strokes, and molecular motors, *Applied Physics A* **75**, 315 (2002).
- [54] E. Brunello, L. Marcucci, M. Irving, and L. Fusi, Activation of skeletal muscle is controlled by a dual-filament mechano-sensing mechanism, *Proceedings of the National Academy of Sciences* **120**, e2302837120 (2023).
- [55] W. Ma, C. L. del Rio, L. Qi, M. Prodanovic, S. Mijailovich, C. Zambataro, H. Gong, R. Shimkunas, S. Golapudi, S. Nag, and T. C. Irving, Myosin in autoinhibited off state(s), stabilized by mavacamten, can be recruited in response to inotropic interventions, *Proceedings of the National Academy of Sciences* **121**, e2314914121 (2024).
- [56] M. Pelishke and B. Bergersen, Equilibrium statistical physics, in *Equilibrium Statistical Physics* (Prentice Hall, Englewood Cliffs, 1989) Chap. 3.